Enhanced Electrochemical Properties of a Novel Polyvinyl Formal Membrane Supporting Gel Polymer Electrolyte by Al$_2$O$_3$ Modification

Yan Wen, Fang Lian, Yan Ren, Hong-Yan Guan

School of Materials Science and Engineering, University of Science and Technology Beijing, Beijing 100083, China
Correspondence to: F. Lian (E-mail: lianfang@mater.ustb.edu.cn)

ABSTRACT: Polyvinyl formal (PVFM)-based dense polymer membranes with nano-Al$_2$O$_3$ doping are prepared via phase inversion method. The membranes and also their performances as gel polymer electrolytes (GPEs) for lithium ion battery are studied by field emission scanning electron microscope, X-ray diffraction, differential scanning calorimetry, mechanical strength test, electrolyte uptake test, electrochemical impedance spectroscopy, cyclic voltammetry, and charge–discharge test. The polymer membrane with 3 wt % nano-Al$_2$O$_3$ doping shows the improved mechanical strength of 12.16 MPa and electrolyte uptake of 431.25% compared with 10.47 MPa and 310.59% of the undoped sample, respectively. The membrane absorbs and swells liquid electrolyte to form stable GPE with ionic conductivity of 4.92×10^{-4} S cm^{-1} at room temperature,

which is higher than 1.77×10^{-4} S cm^{-1} of GPE from the undoped membrane. Moreover, the Al$_2$O$_3$-modified membrane supporting GPE exhibits wide electrochemical stability window of 1.2–4.8 V (vs. Li/Li$^+$) and good compatibility with LiFePO$_4$ electrode, which implies Al$_2$O$_3$-modified PVFM-based GPE to be a promising candidate for lithium ion batteries. © 2014 Wiley Periodicals, Inc. J. Polym. Sci., Part B: Polym. Phys. **2014**, *52*, 572–577

KEYWORDS: additives; aluminum oxide; conducting polymers; crosslinking; differential scanning calorimetry (DSC); electrochemistry; gel polymer electrolyte; gels; membranes; nanocomposites; nanoparticles; phase inversion; polyelectrolytes; phase separation; polyvinyl formal

INTRODUCTION Rechargeable lithium ion battery has been widely accepted as an ideal device for energy storage and conservation due to its high energy density. However, there are some issues in the commercial lithium ion battery, such as potential risk related to leakage and fire of liquid electrolyte. Gel polymer electrolyte (GPE) has been attracting more and more interests because of its higher security than liquid electrolyte.[1] Recently, many GPEs consisting of polymer matrices, plasticizing organic solvents, and lithium salts have been intensively studied to promote their application in lithium ion batteries and other electrochemical devices.[2–4] Although GPEs with high ionic conductivity can usually be achieved by adding large amounts of organic solvents, their mechanical ruggedness is too low to withstand winding and stacking during manufacturing process,[5–7] which is likely to cause internal short-circuiting or thermal runaway of the batteries.[8] These drawbacks of GPEs hinder their industrialization. Membrane supporting GPEs, one of the most promising series, can act simultaneously as transport channel for lithium ions, separator, and binder between anode and cathode.[9] The varied polymer membrane supporting GPEs have been developed recently, including polyethylene oxide (PEO),[10] polyacrylonitrile (PAN),[11] polymethyl methacrylate (PMMA),[12] polyvinylidene

fluoride (PVDF),[13] and poly(vinylidene fluoride-hexafluoropropylene) P(VDF-HFP).[14]

In our previous study, a novel polyvinyl formal (PVFM)-based porous and dense membrane have been prepared via phase inversion method,[15] which remain stable in the commercial electrolyte and form GPEs for Li-ion batteries. The morphology of the polymer membrane was optimized according to the polymer–solvent–nonsolvent ternary phase diagram. Porous membranes are prepared from the region of poor phase nucleation metastable gap, while dense membranes can be synthesized in homogeneous gap. However, mechanical strength of the polymer membrane and conductivity of the corresponding GPE become the two contradictory goals. Though GPE formed by porous PVFM-based membrane shows high ionic conductivity of 1.25×10^{-3} S cm^{-1}, its low mechanical strength of 1.29 MPa needs further improvement for GPEs. We try to improve mechanical strength and thermal retention of PVFM-based porous membrane by coating polyvinyl alcohol (PVA)-Al$_2$O$_3$ solution. The mechanical strength of the membrane is increased from 1.29 MPa to 3.27 MPa and thermal retention is improved from 83% to 97% after storage at 150 °C for 0.5 h, but the ionic conductivity of the corresponding GPE decreases obviously.

While, the dense PVFM-based membrane shows the mechanical strength of 10.47 MPa and the dimensional retention of 93%, but there is a need to further enhance the ionic conductivity of the corresponding GPE of 1.77×10^{-4} S cm^{-1} at room temperature. Incorporation of nanosized particles into the polymer matrix and doping nanoparticles in polymers were performed herein to improve its ionic conductivity. In detail, PVFM-based dense polymer membrane was prepared by doping nano-Al_2O_3 into the polymer matrix by phase inversion process. The inorganic nanoparticle is expected to promote the ionic conductivity due to its high surface area and simultaneously improve the mechanical strength from its connected network with polymer.[16,17] The as-obtained membranes and their GPEs were characterized by field emission scanning electron microscope (FESEM), X-ray diffraction (XRD), differential scanning calorimetry (DSC), mechanical strength test, liquid uptake test, electrochemical impedance spectroscopy, cyclic voltammetry (CV) measurement, and charge–discharge test.

EXPERIMENTAL

Preparation of PVFM-based Polymer Membranes
Nano-Al_2O_3 (α-Al_2O_3, 13 nm, BDKC) ultrasonically dispersed in alcohol for 1 h, and then dried at 100 °C for 24 h. PVFM (M_W: 70,000, Aldrich) powder was dissolved in N-methyl pyrrolidone (NMP, SCRC) to obtain a homogenous solution with the aid of magnetic stirrer. About 3–5 wt % nano-Al_2O_3 powder was added into the above solution under stirring for 30 min. Chemical crosslinking agent 4,4′-diphenylmethane diisocyanate (MDI, Alfa Aesar) was subsequently added into the above solution under stirring for 30 min at 75 °C. The deionized water as the nonsolvent was finally added to precipitate a white micelles, which was continuously stirred until it became a clear and viscous solution. The resulting slurry was coated on the glass plate and immersed in the coagulation bath consisting of NMP and deionized water to precipitate the polymer membrane. The obtained membranes were washed with deionized water, and the residual solution on the surface was removed with filter paper and finally dried under vacuum at 25 °C for 24 h.

Preparation of PVFM-based Gel Polymer Electrolytes
Al_2O_3-modified PVFM-based membranes were punched into disks of 16 mm in diameter. Dropped a small amount of liquid electrolyte (1M $LiPF_6$ in ethylene carbonate (EC)/dimethyl carbonate (DMC) = 3:7 in vol, BICR) to the surface of the polymer membranes in the argon-filled glove box in which the content of water and oxygen are less than 0.5 ppm, and then the liquid electrolyte swelled the polymer chains to form the GPEs.

Test and Characterization
Morphology of Al_2O_3-modified PVFM-based membranes was characterized by FESEM (Carl Zeiss, SUPRA55, Germany). Crystallization performance was observed by XRD (Rigaku, TTRIII, Japan) from 10° to 100° at a scanning rate of 10° min^{-1} at room temperature and also DSC (TA, Q2000, USA)

from −20 °C to 150 °C at a heating rate of 10 °C min^{-1} in argon atmosphere. Mechanical strength measurements were carried out on a tensile testing apparatus (INSTRON, 5567, USA) at a tensile speed of 10 mm min^{-1}, using samples with size of 1 cm × 3 cm at room temperature. In electrolyte uptake measurement, the polymer membrane with size of 16 mm in diameter was immersed in electrolyte solution at 25 °C for 0.5 h. After taking out and slightly absorbing the excessive electrolyte solution at the surface using filter paper, the GPE was weighted and the electrolyte uptake was calculated using the following equation (eq 1)[18]:

$$A(\%) = \frac{W_2 - W_1}{W_1} \times 100 \qquad (1)$$

where W_1 and W_2 are the weight of the membrane and GPE, respectively.

The electrochemical stability of GPE was analyzed by CV with the three-electrode cell containing PVFM-based GPEs, stainless steel (SS, $\varphi = 16$ mm) as working electrode, metallic lithium as counter and reference electrode, respectively. The CV measurement was conducted on an electrochemical work station (CH Instruments, Chi660a, China) with the potential scanning rate of 5 mV S^{-1} from 0 V to 5 V (vs. Li/Li$^+$). The ionic conductivity of GPE was determined using impedance measurement on the symmetrical cell SS/GPE/SS with potential amplitude of 5 mV from 100 kHz to 0.01 Hz. Moreover, Li/LiFePO$_4$ half-cells were assembled for study on the performance of GPEs matching with electrode. The positive electrode was fabricated from 85 wt % LiFePO$_4$ powder as a active material, 10 wt % acetylene black as a conductive additive, and 5 wt % PVDF as a binder. The mixture was stirred and coated onto aluminum foil. The electrode film was dried under vacuum for 24 h at 120 °C to remove any solvent on the electrode surface. Coin cells (CR2032) without separators were assembled and sealed in an argon-filled glove box. For comparison, the coin cell were also assembled using 1M LiPF$_6$ in EC/DMC (3:7 in volume) and polypropylene (PP)/polyethylene (PE)/PP membrane (Celgard 2325) as electrolyte and separator, respectively. Charge and discharge tests were performed galvanostatically between 2.5 and 4.25 V at room temperature at 0.2 C with a battery test system (Jinnuo Wuhan Corp., LAND CT2001A, China).

RESULTS AND DISCUSSION

Morphology of Al_2O_3-modified PVFM-based Membranes
Figure 1 exhibits back-scattered electron images of FESEM for PVFM-based polymer membranes with 3 wt %, 4 wt %, and 5 wt % nano-Al_2O_3 doping, respectively. Al_2O_3 uniformly disperses in the PVFM-based polymer matrix, and the polymer membrane shows dense morphology with nanoscale pores, which contributes to its higher mechanical strength and better stability.
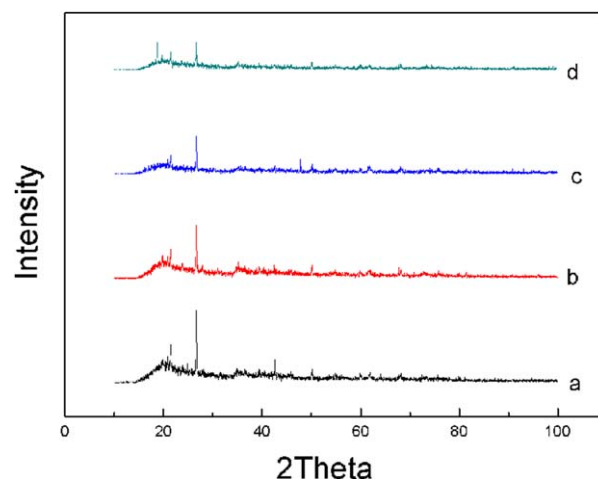
Crystallization Performance
XRD patterns of polymer membranes with different Al_2O_3/PVFM ratio are shown in Figure 2. It can be seen that the
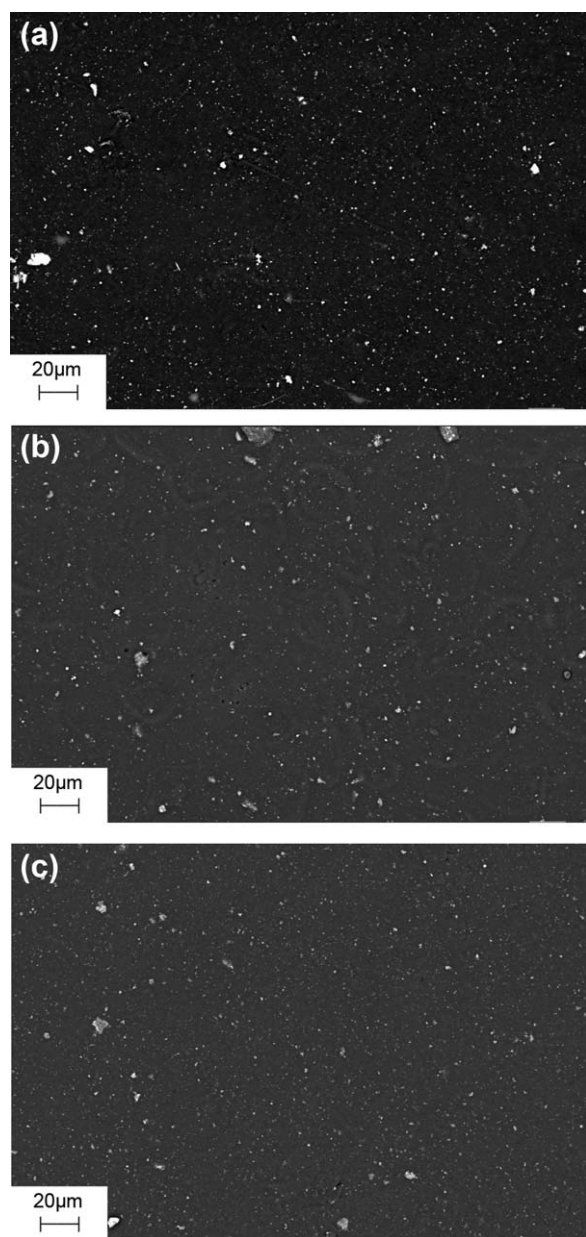
FIGURE 1 FESEM images of polymer membranes with (a) 3 wt %, (b) 4 wt %, and (c) 5 wt % Al$_2$O$_3$ doping.

FIGURE 2 XRD patterns of polymer membranes with (a) 0 wt %, (b) 3 wt %, (c) 4 wt %, and (d) 5 wt % Al$_2$O$_3$ doping. [Color figure can be viewed in the online issue, which is available at wileyonlinelibrary.com.]

crystallinity of the polymer is obviously reduced with increasing nano-Al$_2$O$_3$ doping concentration. The introducing of inorganic powder as a plasticizing agent into polymer matrix can reduce the crystallinity of the polymer, which improves the activity of the polymer chain to the benefit of lithium ions transportation. Meanwhile, the nanosize powder with large specific surface area strengthens surface and interfacial effects to inhibit recrystallization of the polymer and also increases disorder of the polymer chains.

To get information about the transformation of the different phase due to rearrangement of polymer chains upon heating, DSC measurements have been carried out on the polymer membranes. DSC curves of polymer membranes with differ-

ent Al$_2$O$_3$/PVFM ratio are shown in Figure 3. Exothermic peak becomes weaker with Al$_2$O$_3$ particles incorporated into polymer matrix; it indicates that the crystallinity of PVFM matrix is decreased with increasing doping concentration, which leads to an increase in flexibility of the polymer chains.[19]

Mechanical Strength and Electrolyte Uptake

Considering the requirement in the battery manufacture, the mechanical property of a polymer membrane becomes a major character for its use in GPE.[20] Typical stress-deformation curves of PVFM-based membranes with nano-Al$_2$O$_3$ doping are shown in Figure 4. It can be seen from Table 1 that the ultimate tensile strength of PVFM-based dense membrane is 10.47 MPa, and improved by doping Al$_2$O$_3$. PVFM-based membrane with 3 wt % Al$_2$O$_3$ doping
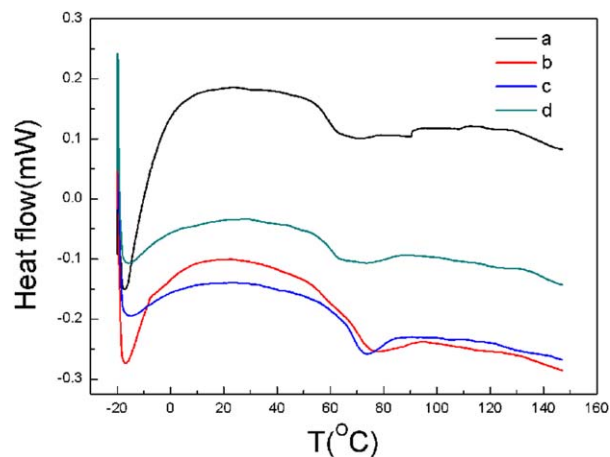
FIGURE 3 DSC curves of polymer membranes with (a) 0 wt %, (b) 3 wt %, (c) 4 wt %, and (d) 5 wt % Al$_2$O$_3$ doping. [Color figure can be viewed in the online issue, which is available at wileyonlinelibrary.com.]
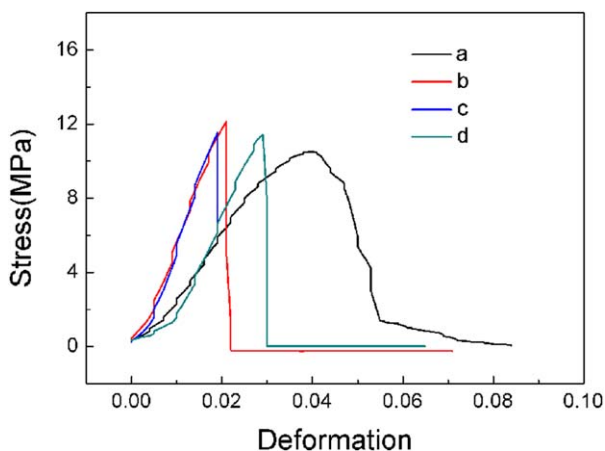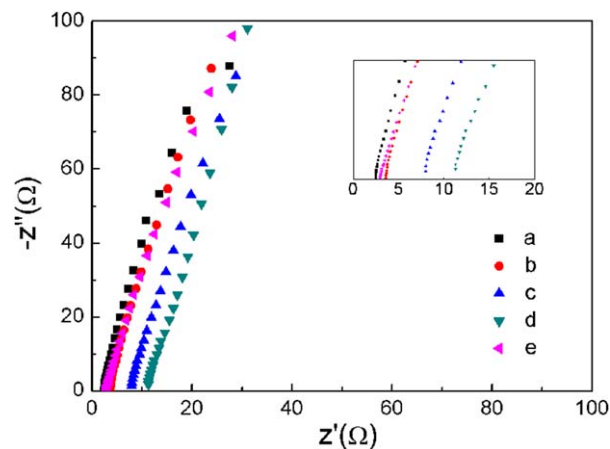
FIGURE 4 The stress-deformation curves of polymer membranes with (a) 0 wt %, (b) 3 wt %, (c) 4 wt %, and (d) 5 wt % Al_2O_3 doping. [Color figure can be viewed in the online issue, which is available at wileyonlinelibrary.com.]

FIGURE 5 Nyquist plots of PVFM-based GPEs with (a) 0 wt %, (b) 3 wt %, (c) 4 wt %, (d) 5 wt % Al_2O_3 doping, and (e) liquid electrolyte with PP/PE/PP membrane. [Color figure can be viewed in the online issue, which is available at wileyonlinelibrary.com.]

shows the highest mechanical property among the samples including the ones with 4 wt % and 5 wt % Al_2O_3 doping. It is deduced that inorganic particles fix polymer chain through hydrogen bonding or van der Waals force and as a result improve mechanical strength of the electrolyte membranes. However, excess inorganic particles will cause a phase separation between polymer and inorganic particles and also bring about voids in the polymer matrix, which results in a decrease in the strength of the membranes. As shown in the stress-deformation curves, the strain value corresponding to the highest stress value of PVFM-based membrane with nano-Al_2O_3 doping is lower than that of PVFM-based dense membrane, which is expected to further improve in the follow-on work.

Table 1 shows electrolyte uptake of PVFM-based polymer membranes. Electrolyte uptake of dense polymer membrane gradually increases with increasing nano-Al_2O_3 content. The uptake values of composite polymer electrolytes are usually greater than those of polymer electrolytes with no filler. The nanoparticles with large surface area can effectively improve the ability for electrolyte retention of the polymer through the capillary force, which contributes to more channels available for migration of lithium ions. The results suggest that nano-Al_2O_3 doping can improve the ionic conductivity of PVFM-based polymer electrolyte.

TABLE 1 The Comparative Characterization on Physicochemical Properties of the Membranes

Sample	Uptake (%)	Conductivity ($\times 10^{-4}$ S cm^{-1})	Strength (MPa)
PVFM (dense)	310.59	1.77	10.47
PVFM-Al_2O_3 (3%)	431.25	4.92	12.16
PVFM-Al_2O_3 (4%)	537.71	4.98	11.54
PVFM-Al_2O_3 (5%)	541.67	5.25	11.44

Ionic Conductivity Behavior

Figure 5 presents the Nyquist plot of the cells at room temperature. The ionic conductivity was calculated from the bulk electrolyte resistance using the following equation (eq 2)[21]:

$$\sigma = \frac{L}{R \cdot S} \qquad (2)$$

where L is the thickness of the GPE, S is the contact area between GPE and SS disc, the bulk electrolyte resistance was obtained from the complex impedance diagram. The ionic conductivity of liquid electrolyte with PP/PE/PP membrane (Celgard 2325) is 4.15×10^{-4} S cm^{-1}. As seen in Table 1, conductivity of PVFM-based GPE is gradually improved with increasing nano-Al_2O_3 content, which is attributed to the decreased crystallinity of the polymer matrix. Moreover, lithium ions can migrate more easily in the PVFM matrix, which is related to the resultant continuous network of favorable lithium ion conduction pathways around the well dispersed nano-Al_2O_3 particles.[22]

Electrochemical Stability

Figure 6 presents the CV curves of PVFM-based GPE with 3 wt % Al_2O_3 doping using Li/GPE/SS cells. Electrochemical stability window of PVFM-based GPE with 3 wt % Al_2O_3 doping is 1.2–4.8 V (vs. Li/Li$^+$), which is similar to the 4 wt % and 5 wt % Al_2O_3 doped GPE. According to previous studies in our lab, electrochemical stability window of PVFM-based GPE is 1.8–5.0 V (vs. Li/Li$^+$),[15] suggesting that nano-Al_2O_3-modified PVFM-based GPE is good enough for the application in the lithium-ion batteries.

Electrode Matching Performance

Figure 7 shows the initial charge and discharge performance of the Li/LiFePO$_4$ half-cells using the GPEs modified by nano-Al_2O_3 at 0.2 C from 2.5 V to 4.25 V at 25 °C. The half-cell of Li/PVFM-based GPE/LiFePO$_4$ with 3 wt % Al_2O_3
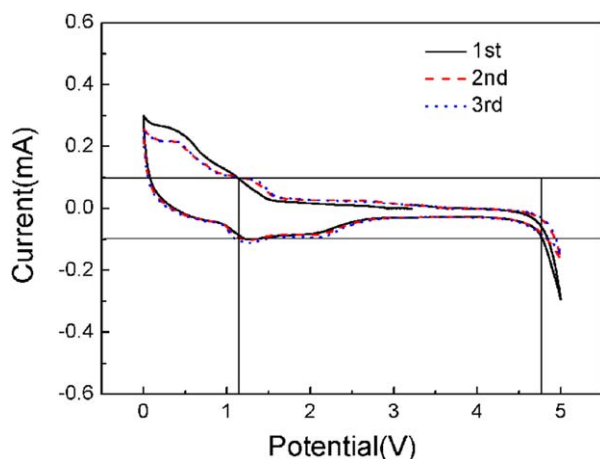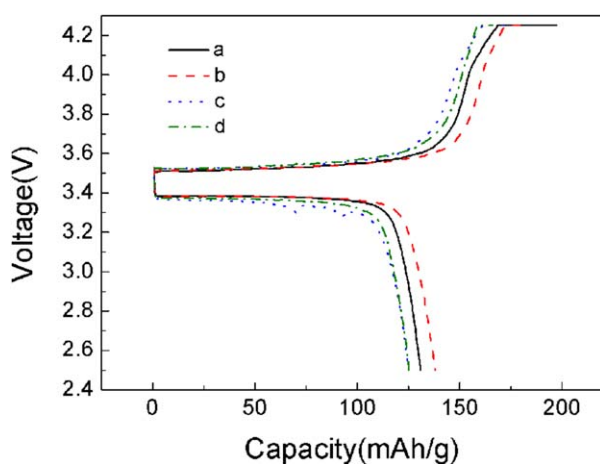
FIGURE 6 The CV curve of PVFM-based GPE with 3 wt % Al_2O_3 doping. [Color figure can be viewed in the online issue, which is available at wileyonlinelibrary.com.]

FIGURE 8 Cyclic stability of Li/liquid electrolyte/$LiFePO_4$ and Li/PVFM-based GPEs/$LiFePO_4$ cells. [Color figure can be viewed in the online issue, which is available at wileyonlinelibrary.com.]
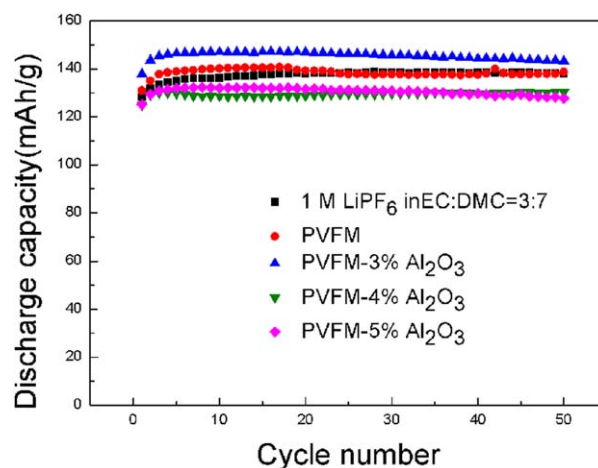
doping shows the smallest polarization and the largest discharge capacity which is better than the cell using PVFM-based GPE without Al_2O_3 doping. Figure 8 presents the cycling performance of the Li/$LiFePO_4$ half-cells prepared with the liquid electrolyte and the PVFM-based GPEs, respectively. The half cell using GPE with 3 wt % Al_2O_3 doping delivers the initial discharge capacity of 137.9 mA hg^{-1} and initial columbic efficiency of 75.4%. The discharge capacity of the cell at 50th cycle is 143.2 mA hg^{-1} and capacity retention is 97.3%. It is indicated that Al_2O_3-modified PVDF-based GPE is therefore a very promising candidate for GPE for lithium-ion batteries.

CONCLUSIONS

PVDF-based dense polymer membranes are modified by doping nano-Al_2O_3 into polymer matrix solution. The mechanical

FIGURE 7 The initial charge–discharge curves of the coin cells Li/PVFM-based GPE doping with (a) 0 wt %, (b) 3 wt %, (c) 4 wt %, and (d) 5 wt % Al_2O_3/$LiFePO_4$ at the 0.2 C rate between 2.5 V and 4.25 V. [Color figure can be viewed in the online issue, which is available at wileyonlinelibrary.com.]

strength and electrolyte uptake of the membrane, the ionic conductivity of the corresponding GPE are improved with uniform nano-Al_2O_3 doping in the PVFM-based polymer to meet the requirements of the electrolyte for lithium ion batteries. The initial tests of Al_2O_3-modified PVFM-based GPEs matched with $LiFePO_4$ show comparable electrochemical performance to the system with liquid electrolyte. Further studies on the application of these membranes in lithium-ion polymer cells are in progress.

REFERENCES AND NOTES

1 Y. Huang, X. Y. Ma, G. Z. Liang, S.H. Wang, Q. L. Zhang, *Polymer* **2008**, *49*, 2085–2094.

2 D. W. Kim, Y. K. Sun, *J. Power Sources* **2001**, *102*, 41–45.

3 H. P. Zhang, P. Zhang, Z. H. Li, M. Sun, Y. P. Wu, H. Q. Wu, *Electrochem. Commun.* **2007**, *9*, 1700–1703.

4 H. Y. Guan, F. Lian, K. Xi, Y. Ren, J. L. Sun, R. V. Kumar, *J. Power Sources* **2014**, *245*, 95–100.

5 S. H. Kim, J. K. Cho, Y. C. Bae, *J. Appl. Polym. Sci.* **2001**, *81*, 948–956.

6 K. M. Abraham, M. Alamgir, D. K. Hoffman, *J. Electrochem. Soc.* **1995**, *142*, 683–687.

7 Y. K. Yarovoy, H. P. Wang, S. L. Wunder, *Solid State Ionics* **1999**, *118*, 301–310.

8 M. Kim, G. Y. Han, K. J. Yoon, J. H. Park, *J. Power Sources* **2010**, *195*, 8302–8305.

9 C. L. Cheng, C. C. Wan, Y. Y. Wang, *J. Power Sources* **2004**, *134*, 202–210.

10 J. L. Wang, J. X. Lei, *J. Polym. Sci. Part B: Polym. Phys.* **2012**, *50*, 656–667.

11 P. Raghavan, J. Manuel, X. H. Zhao, D. S. Kim, J. H. Ahn, C. Nah, *J. Power Sources* **2011**, *196*, 6742–6749.

12 C. H. Kim, H. T. Kim, J. K. Park, S. I. Moon, M. S. Yoon, *J. Polym. Sci. Part B: Polym. Phys.* **1996**, *34*, 2709–2714.

13 J. Saunier, F. Alloin, J. Y. Sanchez, B. Barrière, *J. Polym. Sci. Part B: Polym. Phys.* **2004**, *42*, 532–543.

14 A. M. Elmér, P. Jannasch, *J. Polym. Sci. Part B: Polym. Phys.* **2007**, *45*, 79–90.

15 Y. Ren, F. Lian, Y. Wen, H. Y. Guan, *Polymer* **2013**, *54*, 4807–4813.

16 R. L. Liang, H. Q. Cao, D. Qian, J. X. Zhang, M.Z. Qu, *J. Mater. Chem.* **2011**, *21*, 17654–17657.

17 F. Zhang, H. Q. Cao, D. M. Yue, J. X. Zhang, M.Z. Qu, *Inorg. Chem.* **2012**, *51*, 9544–9551.

18 H. S. Min, D. W. Kang, D. Y. Lee, D. W. Kim, *J. Polym. Sci. Part B: Polym. Phys.* **2002**, *40*, 1496–1502.

19 N. T. Kalyana Sundaram, A. Subramania, *Electrochim Acta* **2007**, *52*, 4987–4993.

20 C. L. Cheng, C. C. Wan, Y. Y. Wang, M. S. Wu, *J. Power Sources* **2005**, *144*, 238–243.

21 Y. H. Liao, X. P. Li, C. H. Fu, R. Xu, M.M. Rao, L. Zhou, S.J. Hu, W. S. Li, *J. Power Sources* **2011**, *196,* 6723–6728.

22 J. Cao, L. Wang, X. M. He, M. Fang, J. Gao, J. J. Li, L. F. Deng, H. Chen, G. Y. Tian, J. L. Wang, S. S. Fan, *J. Mater. Chem. A* **2013**, *1*, 5955–5961.